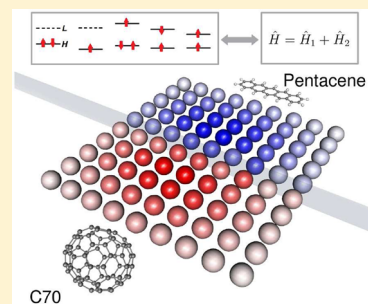


# An Effective Two-Orbital Quantum Chemical Model for Organic Photovoltaic Materials

Guido Raos,\* Mosè Casalegno, and Julien Idé

Dipartimento di Chimica, Materiali e Ingegneria Chimica "G. Natta", Politecnico di Milano, via L. Mancinelli 7, 20131 Milano, Italy

**ABSTRACT:** We present a coarse-grained quantum chemical model of organic photovoltaic materials, which is based on the classic idea that the main physical processes involve the electrons occupying the frontier orbitals (HOMO and LUMO) of each molecule or "site". This translates into an effective electronic Hamiltonian with two electrons and two orbitals per site. The on-site parameters (one- and two-electron integrals) can be rigorously related to the ionization energy, electron affinity, and singlet and triplet first excitation energies of that site. The intersite Hamiltonian parameters are introduced in a way that is consistent with classical electrostatics, and for the one-electron part, we use a simple approximation that could be refined using information from atomistic quantum chemical calculations. The model has been implemented within the GAMESS-US package. This allows the exploration of the physics of these materials using state-of-the-art quantum chemical methods on relatively large systems (hundreds of electron-donor and electron-acceptor sites). To illustrate this point, we present ground- and excited-state calculations on dimers and two-dimensional arrays of sites using the Hartree–Fock, configuration interaction, and coupled-cluster methods. The calculations provide evidence for the possibility of low-energy, long-range electron transfer in donor–acceptor heterojunctions characterized by a moderate degree of disorder.



## I. INTRODUCTION

Organic photovoltaic devices have undergone tremendous development over the past decade, as testified by their steady approach to the 10% power conversion efficiency that is often considered necessary for their large-scale deployment.<sup>1</sup> This progress has been possible thanks to the development of new electron-acceptor (A) and electron-donor (D) materials, new electrodes, new device assembly procedures, careful control of the structure and morphology of the D–A blends, and last but not least, a better understanding of the physics of these devices. Even so, there are still significant gaps in our fundamental knowledge of their inner workings. It is a real challenge to understand the nature and evolution of the electronic states in these systems, which are characterized by high chemical heterogeneity (polymers, oligomers, and small molecules, but also inorganic semiconductors and metals), different degrees of thermal and structural disorder, complex morphologies, and diffuse interfaces.<sup>2</sup>

In order to shed some light on these complex materials and devices, a growing number of workers have undertaken their study from a theoretical or computational perspective.<sup>3</sup> Some people have carried out atomistic<sup>4</sup> or coarse-grained<sup>5</sup> molecular dynamics simulations of D–A blends. Snapshots from these simulations have been sometimes used as an input to subsequent quantum mechanical or classical (microelectrostatic) calculations of interface energetics and electronic states.<sup>3,4</sup> Unfortunately, these approaches can be extremely expensive, and it could be argued that even when they are applied to their full power they are not yet ready to capture the structural and morphological complexities of real devices.<sup>6</sup> In parallel, others have approached the simulation of whole photovoltaic devices using coarser and more phenomeno-

logical methods, such as kinetic Monte Carlo (KMC),<sup>7</sup> master equation (ME)<sup>8</sup> or drift-diffusion (DD)<sup>9</sup> simulations. Often, also these have been applied on somewhat idealized systems, but more recently, there have been interesting attempts to combine them with more realistic models of phase-separating polymer blends.<sup>10</sup> These simulations, however, suffer from the fundamental shortcoming of being rooted in "classical" descriptions of the excitons and charge carriers. This implies, for example, that these quasi-particles are simply assumed to be localized and to diffuse by a hopping mechanism. Also, such classical models cannot account for the electron spin. This is an important shortcoming, due to the growing interest in increasing device efficiencies by exploiting "singlet fission".<sup>11</sup>

The previous discussion demonstrates, in our opinion, that there is a real need for a theoretical and computational model covering the middle ground between atomistic quantum chemical descriptions (density functional or semiempirical molecular orbital theories are the only viable options, given the complexity of these systems) and more phenomenological approaches (KMC, ME, and DD). To be useful, such a method should generate semiquantitative results and, equally important, qualitative insights. Our purpose here is to propose such a method. The approach is similar in spirit but different in detail from that of Troisi,<sup>12</sup> who recently studied the generation of free charges at D–A interfaces from the perspective of electron transfer theory. It is an approximate but truly many-body approach, as it avoids the one-electron approximation of Hückel-like models (see also a recent paper on this topic<sup>13</sup>). It

**Received:** September 28, 2013

is consistent with classical electrostatics, but unlike it, it does not assume charge (or wave function) localization.

Sections II–IV contain a description of the basic physical model and the development of the necessary theory, first for isolated molecules and then for many interacting ones. Section V contains our first applications. These are not meant to provide a comprehensive set of results but rather to illustrate the kind of insights that can be obtained by application of the model. Conclusions follow.

## II. THE MODEL

Let us consider an assembly of  $M$  sites, which may represent whole  $\pi$ -conjugated molecules ( $C_{60}$  and its derivatives, acenes, phthalocyanines, etc.), the conjugated fragments within some long polymer chains (polythiophenes or some of the new generation copolymers) or as in some lattice models of organic photovoltaic devices, they may be just a conventional discretization of the material without any reference to well-defined molecular features. For simplicity, from now on, the terms site and molecule will be used interchangeably. The sites are assumed to be roughly isotropic, so their configuration is entirely specified by the center-of-mass coordinates  $\mathbf{R}_i$  ( $i = 1, 2, \dots, M$ ). We also neglect all dynamical phenomena associated with the nuclear degrees of freedom (incidentally, Troisi<sup>12</sup> has recently pointed that nuclear motions might be unimportant for charge separation at the D–A interface). Hence, the site coordinates may be simply assumed to be fixed. On each site  $i$ , there are two basis functions, a “highest occupied molecular orbital” (HOMO) and a “lowest unoccupied molecular orbital” (LUMO), respectively,  $\phi_{2i-1}(\mathbf{r})$  and  $\phi_{2i}(\mathbf{r})$ . In its ground state, each site has two electrons within the HOMO orbital. Thus, there are  $2M$  orbitals and  $2M$  electrons overall.

The orbitals are assumed to be real, normalized, and orthogonal

$$\int \phi_k(\mathbf{r})\phi_l(\mathbf{r})d\mathbf{r} = \delta_{kl} \quad (k, l = 1, \dots, 2M) \quad (1)$$

The orthogonality approximation could be justified on the basis of the smallness of the overlap integral between the orbitals on two distinct molecules (the HOMO and LUMO on the same site would be orthogonal anyway), or by assuming that the  $\phi_k$  values have been obtained from the unperturbed orbitals of the isolated molecules through an intermediate symmetric (Löwdin) orthogonalization step.<sup>14</sup> In any case, by making this approximation, we follow the path traced by many semi-empirical molecular electronic structure theories or by the Hubbard model in solid-state physics.<sup>15,16</sup> In fact, below we shall adopt an INDO-like (intermediate neglect of differential overlap<sup>15,16</sup>) approximation, whereby all two-electron integrals involving a product between orbitals on different sites are neglected.

In our local orthogonal orbital basis, the nonrelativistic electronic Hamiltonian may be written in second quantization form<sup>14,16</sup>

$$\begin{aligned} \hat{H} &= \hat{H}_1 + \hat{H}_2 \\ &= \sum_{i,j=1}^{2M} \sum_{\sigma=\alpha}^{\beta} h_{ij} a_{i\sigma}^{\dagger} a_{j\sigma} + \frac{1}{2} \sum_{i,j,k,l=1}^{2M} \sum_{\sigma,\tau=\alpha}^{\beta} c_{ijkl} a_{i\sigma}^{\dagger} a_{j\tau}^{\dagger} a_{l\tau} a_{k\sigma} \end{aligned} \quad (2)$$

where  $\sigma$  and  $\tau$  are electron spin coordinates, and  $a_{i\sigma}^{\dagger}$  and  $a_{i\tau}$  are electron creation and annihilation operators satisfying the usual

fermion anticommutation rules, respectively. The one- and two-electron integrals entering the Hamiltonian are (in atomic units)<sup>18</sup>

$$h_{ij} = \int \phi_i(\mathbf{r}) \left[ -\frac{1}{2} \nabla^2 - \sum_{k=1}^M \frac{Z_k}{|\mathbf{r} - \mathbf{R}_k|} \right] \phi_j(\mathbf{r}) d\mathbf{r} \quad (3)$$

$$c_{ijkl} = \int \int \phi_i(\mathbf{r}_1) \phi_k(\mathbf{r}_1) \frac{1}{|\mathbf{r}_1 - \mathbf{r}_2|} \phi_j(\mathbf{r}_2) \phi_l(\mathbf{r}_2) d\mathbf{r}_1 d\mathbf{r}_2 \quad (4)$$

All the physics of the system is contained in these one- and two-electron integrals. Our first task will be to derive simple but physically sound approximations and parametrization schemes for them.

## III. ON-SITE HAMILTONIAN AND ELECTRONIC STATES

We first consider the parametrization of the on-site integrals. Given a single molecule, we may refer to its HOMO and LUMO orbitals simply as  $\phi_1$  and  $\phi_2$  (we will resume the full notation later on). This two-orbital system may be occupied by two electrons (neutral molecule), but we are also interested in describing situations with one or three electrons (molecular cation and anion, respectively). The main electronic states, which are expected to be relevant for organic photovoltaic materials, are depicted in Figure 1. Their wave functions may be

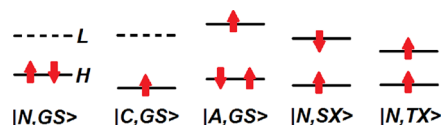


**Figure 1.** Main electronic states for a two-orbital site occupied by one, two, or three electrons. H and L stand HOMO and LUMO orbitals, respectively. The latter is represented by a dashed line when it is unoccupied or “virtual”. The orbital energies depend on the state to indicate that our model goes beyond the independent particle picture by including electron–electron interactions.

written using Slater determinants or in second quantization through the action of the electron creation operators on the vacuum state  $|0\rangle$ .<sup>14,16</sup> We have for the ground state of the neutral molecule

$$|N,GS\rangle = \frac{1}{\sqrt{2}} |\phi_1(1)\alpha(1)\phi_1(2)\beta(2)| = a_{1\alpha}^{\dagger} a_{1\beta}^{\dagger} |0\rangle \quad (5)$$

and for the ground state of the cation

$$|C,GS\rangle = \phi_1(1)\alpha(1) = a_{1\alpha}^{\dagger} |0\rangle \quad (6)$$

and for the ground state of the anion

$$\begin{aligned} |A,GS\rangle &= \frac{1}{\sqrt{6}} |\phi_1(1)\alpha(1)\phi_1(2)\beta(2)\phi_2(3)\alpha(3)| \\ &= a_{1\alpha}^{\dagger} a_{1\beta}^{\dagger} a_{2\alpha}^{\dagger} |0\rangle \end{aligned} \quad (7)$$

and for the singly excited singlet state of the neutral molecule

$$\begin{aligned} |N,SX\rangle &= \frac{1}{2} \{ |\phi_1(1)\alpha(1)\phi_2(2)\beta(2)| \\ &\quad - |\phi_1(1)\beta(1)\phi_2(2)\alpha(2)| \} \\ &= \frac{1}{\sqrt{2}} \{ a_{1\alpha}^{\dagger} a_{2\beta}^{\dagger} - a_{1\beta}^{\dagger} a_{2\alpha}^{\dagger} \} |0\rangle \end{aligned} \quad (8)$$

and finally, for the singly excited triplet state of the neutral molecule

$$\begin{aligned} |N, TX\rangle &= \frac{1}{2} \{ |\phi_1(1)\alpha(1)\phi_2(2)\beta(2)| \\ &\quad + |\phi_1(1)\beta(1)\phi_2(2)\alpha(2)| \} \\ &= \frac{1}{\sqrt{2}} \{ a_{1\alpha}^\dagger a_{2\beta}^\dagger + a_{1\beta}^\dagger a_{2\alpha}^\dagger \} |0\rangle \end{aligned} \quad (9)$$

Notice that we have neglected configuration mixing, in particular the possible contribution of the doubly excited configuration to  $|N, GS\rangle$ . This is a reasonable approximation for well-separated HOMO and LUMO levels, as will be shown below when we come to the numerical tests of the theory. The energies of these electronic states can be obtained by straightforward application of Slater's rules or of the algebra of the second-quantized operators<sup>14,16</sup>

$$E_{|N, GS\rangle} = 2h_{11}^0 + c_{1111} \quad (10)$$

$$E_{|C, GS\rangle} = h_{11}^0 \quad (11)$$

$$E_{|A, GS\rangle} = 2h_{11}^0 + h_{22}^0 + c_{1111} + 2c_{1122} - c_{1221} \quad (12)$$

$$E_{|N, SX\rangle} = h_{11}^0 + h_{22}^0 + c_{1122} + c_{1221} \quad (13)$$

$$E_{|N, TX\rangle} = h_{11}^0 + h_{22}^0 + c_{1122} - c_{1221} \quad (14)$$

We have added a 0 superscript to the one-electron integrals, as these will be corrected below to account for the interaction with the other molecules.

We now assume to have at our disposal (from accurate gas-phase experiments and/or ab initio calculations, but for some purposes even an “educated guess” should be adequate) the ionization energy (IE), electron affinity (EA), and singlet and triplet excitation energies of the molecule (SX, TX, respectively). These four experimental data are in principle insufficient to determine the six parameters entering the on-site Hamiltonian, but the latter can be reduced in number by assuming that all Coulomb integrals have similar values

$$c_{1111} \simeq c_{1122} \simeq c_{2222} \quad (15)$$

This approximation is reasonable when the HOMO and LUMO orbitals have comparable spatial extents and they are roughly located within the same region of the molecule.<sup>19</sup> For large molecules, these conditions are quite compatible with the orthogonality of  $\phi_1$  and  $\phi_2$ . Instead,  $c_{1221}$  is fundamentally different from the other three integrals because it represents an exchange interaction. Together with the one-electron “hopping” integrals to be discussed below, these exchange integrals are the only terms in the Hamiltonian with a nonzero differential overlap. Their presence is essential in order to produce a splitting between the excited singlet and triplet states. Subtracting eq 10 from eqs 11–14 and rewriting everything as a matrix equation, we find

$$\begin{bmatrix} \text{IE} \\ \text{EA} \\ \text{SX} \\ \text{TX} \end{bmatrix} = \begin{bmatrix} -1 & 0 & -1 & 0 \\ 0 & -1 & -2 & 1 \\ -1 & 1 & 0 & 1 \\ -1 & 1 & 0 & -1 \end{bmatrix} \begin{bmatrix} h_{11}^0 \\ h_{22}^0 \\ c_{1111} \\ c_{1221} \end{bmatrix} \quad (16)$$

The on-site Hamiltonian parameters can be obtained as a function of the experimental data by a simple matrix inversion:

$$\begin{bmatrix} h_{11}^0 \\ h_{22}^0 \\ c_{1111} \\ c_{1221} \end{bmatrix} = \begin{bmatrix} -2 & 1 & 0 & 1 \\ -2 & 1 & 1/2 & 3/2 \\ 1 & -1 & 0 & -1 \\ 0 & 0 & 1/2 & -1/2 \end{bmatrix} \begin{bmatrix} \text{IE} \\ \text{EA} \\ \text{SX} \\ \text{TX} \end{bmatrix} \quad (17)$$

Table I demonstrates the application of our procedure on  $C_{70}$ <sup>20,21</sup> and pentacene,<sup>22</sup> respectively, taken as typical electron-

**Table I. Gas-Phase Experimental Data<sup>20,22</sup> and On-Site Hamiltonian Parameters for  $C_{70}$  and Pentacene ( $C_{22}H_{14}$ )<sup>a</sup>**

	data (eV)		parameters ( $E_h$ )		
	$C_{70}$	$C_{22}H_{14}$		$C_{70}$	$C_{22}H_{14}$
IE	7.48	6.61	$h_{11}^0$	−0.3939	−0.3715
EA	2.68	1.35	$h_{22}^0$	−0.3204	−0.2973
SX	2.44	2.28	$c_{1111}$	0.1191	0.1286
TX	1.56	1.76	$c_{1221}$	0.0162	0.0096

<sup>a</sup>One Hartree is  $E_h = 27.211$  eV.

acceptor (A) and electron-donor (D) materials. Overall, the parameters take “reasonable” values with  $h_{11}^0 < h_{22}^0 \ll 0$  (the values *seem* to be small because they are given in atomic units!) and  $c_{1111} \gg c_{1221} > 0$ . At the same time, notice how the very significant differences between the electronic properties of  $C_{70}$  and pentacene translate into very subtle differences in their Hamiltonians. The on-site Coulomb integrals are especially interesting as their values should be roughly related to the spatial extent of the HOMO and LUMO orbitals, which are identical in the approximation of eq 15. Assuming for simplicity a spherical Gaussian charge distribution

$$\rho_1(\mathbf{r}) = -\phi_1^2(\mathbf{r}) = -\left(\frac{2\alpha_1}{\pi}\right)^{3/2} e^{-2\alpha_1|\mathbf{r}-\mathbf{R}|^2} \quad (18)$$

its self-repulsion integral is

$$c_{1111} = \iint \frac{\rho_1(\mathbf{r}_1)\rho_1(\mathbf{r}_2)}{|\mathbf{r}_1 - \mathbf{r}_2|} d\mathbf{r}_1 d\mathbf{r}_2 = \sqrt{\frac{4\alpha_1}{\pi}} \quad (19)$$

We may reverse this equation to obtain an estimate of the spatial extent (the standard deviation)  $\sigma_1$  of the charge distribution from the integral

$$\sigma_1 = \sqrt{\frac{3}{4\alpha_1}} = \sqrt{\frac{3}{\pi}} \frac{1}{c_{1111}} \quad (20)$$

Substituting the values in Table I, we obtain  $\sigma_1 = 8.20$ ,  $a_0 = 4.34$  Å for  $C_{70}$ ,  $\sigma_1 = 7.60$ , and  $a_0 = 4.02$  Å for pentacene, which are rightly comparable to the actual size of these molecules (the Bohr radius is  $a_0 = 0.52918$  Å).

#### IV. EXTENSION TO MANY MOLECULES

Let us proceed to discuss the electronic Hamiltonian for a system containing several molecules (we now switch back to the full notation for the orbital indices). As mentioned above, we adopt a minimalist INDO-type approach, essentially retaining only those “classical” terms that are strictly necessary in order to describe a system of interacting charges. First of all, the on-site one-electron Hamiltonian must be modified in order to account for the Coulomb attraction by the positively charged cores of the other molecules. The LUMO–LUMO matrix elements become

$$h_{2i,2i} = h_{2i,2i}^0 + w_{2i} - \sum_{k \neq i}^M \int \frac{Z_k \phi_{2i}^2(\mathbf{r})}{|\mathbf{r} - \mathbf{R}_k|} d\mathbf{r} \quad (21)$$

and similarly for the HOMO–HOMO ones ( $h_{2i-1,2i-1}$ ). The on-site HOMO–LUMO elements are absent in the isolated molecules<sup>17</sup> ( $h_{2i-1,2i}^0 = 0$ ), and they will be neglected also in the many-molecule system, consistent with our INDO-type approach. On the right-hand side of eq 21,  $w_{2i}$  is an optional term accounting for “diagonal” or “energetic” disorder. It is a random number drawn from a Gaussian distribution with a mean of zero and a standard deviation,  $\sigma_w$ , going from zero (in which case  $w_{2i} \equiv 0$ ) to more than 0.1 eV for a very disordered material<sup>23</sup> (for comparison, the thermal energy is  $k_B T = 0.026$  eV at room temperature). Next, we approximate the integrals on the right-hand side by the electrostatic interaction between a Gaussian charge distribution at  $\mathbf{R}_k$  (with overall charge  $Z_k; = +2.0$ ) and a negative Gaussian charge at  $\mathbf{R}_i$  (see eq 18)

$$-\int \frac{Z_k \phi_{2i}^2(\mathbf{r})}{|\mathbf{r} - \mathbf{R}_k|} d\mathbf{r} \simeq -\frac{2.0 \text{erf}(\nu_{2i,k} R_{ik})}{R_{ik}} \quad (22)$$

where  $\text{erf}(x)$  is the error function and  $R_{ik} = |\mathbf{R}_i - \mathbf{R}_k|$ , while

$$\nu_{2i,k} = \sqrt{\frac{2\alpha_{2i}\alpha_{2k-1}}{\alpha_{2i} + \alpha_{2k-1}}} \quad (23)$$

This approximation—in particular the definition of  $\nu_{2i,k}$ —relies on the assumption that the positive charge at  $\mathbf{R}_k$  is not pointlike (a bare nucleus),<sup>18</sup> but it has an extension related the HOMO–HOMO electron repulsion on that site (see eq 19). The rationale is that after removing two electrons from a HOMO orbital we are essentially left with a positive charge distribution that is the “negative image” of that orbital. Notice also that because  $\text{erf}(x) \simeq 1$  for  $x \geq 2$ , these integrals reduce to the ordinary Coulomb interaction between two point charges whenever  $R_{ik} \gtrsim 2\nu_{2i,k}^{-1}$ , i.e., when the superposition between the associated charge distributions becomes negligible.

To complete the one-electron Hamiltonian, we need the “hopping” integrals that couple the orbitals on neighboring sites. In principle, these can be evaluated by a variety of quantum chemical approaches, starting from a detailed atomistic model of the molecules and their mutual arrangement.<sup>24</sup> This possibility will be included in future applications of the model. For the time being, we adopt a simple approximation, inspired by the results of other studies of charge transport in organic semiconductors.<sup>25</sup> For two orbitals  $i$  and  $j$  centered on two sites at a distance  $R_{ij}$ , we take

$$h_{ij} = t_{ij} e^{-(R_{ij}-R_0)/D} \quad (24)$$

where  $t_{ij}$  represents the strength of the coupling between sites at a distance  $R_0$  (the nearest-neighbor distance) and  $D$  determines the spatial range of these couplings. The  $t_{ij}$  values are random numbers drawn from a Gaussian distribution with a mean  $t_0$  and a standard deviation  $\sigma_t$ . The latter can take a value going from zero (for a crystalline material at low temperatures) up to a value comparable or even larger than  $t_0$  (for an amorphous material or even a crystalline one at high temperatures).<sup>25</sup> In principle, all these parameters ( $t_0$ ,  $\sigma_t$ , and  $D$ ) could depend both on molecule types (D–D, D–A, and A–A pairs) and on orbital types (HOMO–HOMO, HOMO–LUMO, and LUMO–LUMO pairs) and, similarly, for the  $\sigma_w$  values, which control the extent of diagonal disorder. Thus, judging from the size of its parameter space, we see that even

our minimalist model is actually quite rich and could be used to describe a variety of physical situations.

Finally, the intersite two-electron integrals are given by

$$c_{ikjl} = \delta_{ik} \delta_{jl} c_{ijij} \quad (25)$$

$$c_{ijij} = \iint \frac{\phi_i^2(\mathbf{r}_1) \phi_j^2(\mathbf{r}_2)}{|\mathbf{r}_1 - \mathbf{r}_2|} d\mathbf{r}_1 d\mathbf{r}_2 \simeq \frac{\text{erf}[\mu_{ij} R_{ij}]}{R_{ij}} \quad (26)$$

where  $\mu_{ij} = (2\alpha_i \alpha_j / (\alpha_i + \alpha_j))^{1/2}$ . Again, notice that the properties of the  $\text{erf}()$  function imply that  $c_{ijij} \simeq 1/R_{ij}$  for  $R_{ij} > 2\mu_{ij}^{-1}$  and, taking  $\alpha_i = \alpha_j$ , we find that  $c_{ijij} \rightarrow c_{iiii}$  (the related on-site Coulomb integral) when  $R_{ij} \rightarrow 0$ . Thus, eq 26 interpolates nicely between the expected long- and short-range behavior.

So far, the theory has been developed under the implicit assumption that all the interactions occur in vacuo. This would indeed be appropriate for an all-electron ab initio approach. However, ours is a semiempirical model in which most of the electrons are implicit, as they reside in lower-than-HOMO orbitals. As such, they are essentially inactive, except for the fact they provide a dielectric medium that can be polarized by electric fields and charges. To take account of this effect, all the intersite interactions (eq 22 for electron–nuclear and eq 26 for electron–electron, plus of course the nuclear repulsion energy) must be simply rescaled by the relative permittivity  $\epsilon_r$ . Here, we take  $\epsilon_r = 3.5$ , which is a typical value for nonpolar organic materials. Also, the on-site Hamiltonian parameter must be modified to take account of the dielectric surrounding the molecules. A polarization-corrected set of data to be fed into eq 17 could be calculated by ab initio calculations within a polarizable continuum medium,<sup>26</sup> but here, we take a simpler approach. For a first approximation, only the charged states (cation and anion) will be affected.<sup>27</sup> The size of the effect can be estimated with the Born formula for the (free) energy of solvation of a charge  $q$  of radius  $r_B$ <sup>28</sup>

$$W = -\frac{q^2}{2r_B} \left( 1 - \frac{1}{\epsilon_r} \right) \quad (27)$$

Using  $q = \pm 1$  and radius  $r_B = 5.0 \text{ \AA} = 9.45 a_0$ , we obtain  $|W| = 0.0378 E_h = 1.03 \text{ eV}$ . This is a significant contribution that decreases the ionization energy and increases the electron affinity compared to the gas-phase values

$$\text{IE}(\text{dielec}) = \text{IE}(\text{gas}) - |W| \quad (28)$$

$$\text{EA}(\text{dielec}) = \text{EA}(\text{gas}) + |W| \quad (29)$$

These polarization-corrected IE and EA values can be inserted into eq 17 to obtain a new set of on-site Hamiltonian parameters. The results are given in Table II. Notice that  $r_B$  has been taken equal to half the nearest-neighbor intersite spacing

**Table II. Polarization-Corrected Data and On-Site Hamiltonian Parameters for C<sub>70</sub> and Pentacene (C<sub>22</sub>H<sub>14</sub>)<sup>a</sup>**

	data (eV)		parameters ( $E_h$ )		
	C <sub>70</sub>	C <sub>22</sub> H <sub>14</sub>	C <sub>70</sub>	C <sub>22</sub> H <sub>14</sub>	
IE	6.45	5.58	$h_{11}^0$	−0.2806	−0.2581
EA	3.71	2.38	$h_{22}^0$	−0.2071	−0.1839
SX	2.44	2.28	$c_{1111}$	0.0435	0.0530
TX	1.56	1.76	$c_{1221}$	0.0162	0.0096

<sup>a</sup>The calculation assumes a relative permittivity  $\epsilon_r = 3.5$  and a Born radius  $r_B = 5.0 \text{ \AA}$  for both materials.



(see calculations below), but it is also comparable to the  $\sigma_i$  values derived from the on-site Coulomb integrals (eq 20). This seems to be an important condition for a sensible semiquantitative application of the model.

## V. APPLICATIONS

We have implemented our model within the GAMESS-US code.<sup>29</sup> In essence, we simply had to code a few routines that replace the ab initio one- and two-electron integrals by the semiempirical ones entering our effective Hamiltonian (eq 2). This implementation allows us to explore the properties of the model using any of the wave function-based—as opposed to density functional-based—ground- and excited-state methods that are already available within GAMESS-US. Below, we present two sets of calculations, first on a donor–acceptor pair and then on two-dimensional model heterojunctions.

As a first application of the model, we have computed the ground and excited states of a donor (D) and an acceptor (A) at different separations. Their on-site parameters are those of pentacene and  $C_{70}$ , respectively, either in vacuo (Table I) or within a dielectric medium (Table II). For the intersite one-electron Hamiltonian, we have taken  $t_0 = 0.08$  eV for the HOMO–HOMO coupling,  $t_0 = 0.00$  eV for the HOMO–LUMO coupling, and  $t_0 = -0.08$  eV for the LUMO–LUMO coupling. Notice that the actual couplings depend on the D–A separation according to eq 24, with  $R_0 = 10.0$  Å and  $D = 3.5$  Å. These values are somewhat arbitrary, but their orders of magnitudes are comparable with those expected for many organic materials.<sup>24,25</sup> We have not included any disorder in this series of calculations ( $\sigma_w = \sigma_t = 0.00$  eV). Figure 2 shows

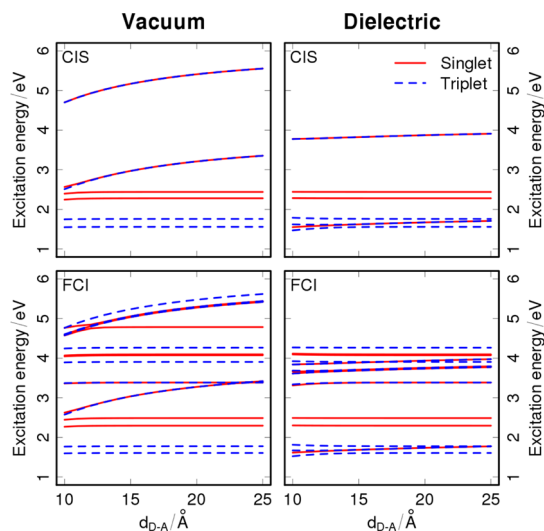


**Figure 2.** Potential energy curves for the interaction of an A and a D site, both in in vacuo (left) and in a dielectric (right), calculated with the CIS (top) or the FCI (bottom) methods.

the singlet and triplet excitation energies computed by configuration interaction calculations including only single excitations (CIS method)<sup>30</sup> or in the full version (FCI),<sup>31</sup> which for this system includes up to quadruple excitations. The FCI method obviously produces more states than CIS (there are also quintet and septet states, which have not been plotted for clarity), but there is excellent agreement between them for the lowest lying ones. The excitation energies at long-range correspond exactly to those of the isolated monomers in Tables

I and II. In the vacuum calculations, the curves for the fifth and sixth excited states are almost perfectly overlapping, and they correspond to  $(D^+)...(A^-)$  charge transfer states, which may have either singlet or triplet spin multiplicities. They have a clear  $1/R$  dependence, in agreement with this interpretation. Much higher in energy, there are analogous curves for the  $(D^-)...(A^+)$  states. In between, the FCI method provides additional roots with double or multiple excited character. Figure 2 shows the Mulliken (or Löwdin, because the orbitals are orthogonal) charges on the D molecule in the lowest lying states. The ground state ( $S_0$ ) is almost perfectly neutral at all distances, while the first excited singlet state ( $S_1$ ) acquires a moderate charge transfer character at the contact distance ( $R_0 = 10$  Å). This charge transfer character would increase with larger interorbital couplings. Instead, the first triplet state ( $T_1$ ) is everywhere neutral because the larger energy separation between the (diabatic) neutral and ionic triplet states prevents a significant mixing between them.

In a dielectric medium (Figure 3, right panel), the energies of the neutral states are virtually unchanged, while those of the

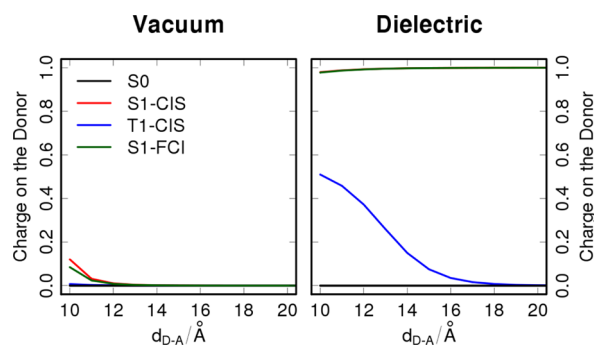


**Figure 3.** Distance dependence of the site charges in the ground ( $S_0$ ) and lowest excited states ( $S_1$ ,  $T_1$ ) of an A–D pair. In the left-hand panel (vacuum), the  $T_1$ –CIS curve is underneath the  $S_0$  one. In the right-hand panel (dielectric), the  $S_1$ –CIS curve is underneath the  $S_1$ –FCI one.

charge-transfer ones are shifted downward and flattened, as expected. The ground state remains neutral, while the  $S_1$  state becomes entirely ionic at all distances (see the charges in Figure 3). This occurs because, according to our Born-type approximation,  $IE(C_{22}H_{14}) - AE(C_{70}) < SX(C_{22}H_{14}) < SX(C_{70})$  (Table II). Hence, in a dielectric, it takes less energy to transfer one electron from D to A than to excite one of them. The  $T_1$  state also becomes partly ionic at short distances when the  $(D^+)...(A^-)$  triplet curve “crosses” the neutral one at  $R \approx 15$  Å.

As a second example, we discuss a series of HF (Hartree–Fock), CIS, and CCSD (coupled-cluster with single and double excitations)<sup>32</sup> calculations on two-dimensional model heterojunctions made up of 15 A and 15 D sites. Figure 4 illustrates their structure, with the sites colored according to their ground-state charges (see below). For comparison, we have also done calculations on analogous systems consisting only of A or D sites. The sites are placed on a regular square lattice, with a spacing of 1.0 nm. This distance is compatible with the actual size of our model D and A molecules (see also the  $\sigma_i$  values obtained from the  $c_{iiii}$  integrals) and with HOMO and LUMO density-of-states (DOS) on the order of  $1/\text{nm}^3$ , which are typical of many photovoltaic materials.<sup>2</sup> We have considered completely ordered D and A phases (oo-case, where the first

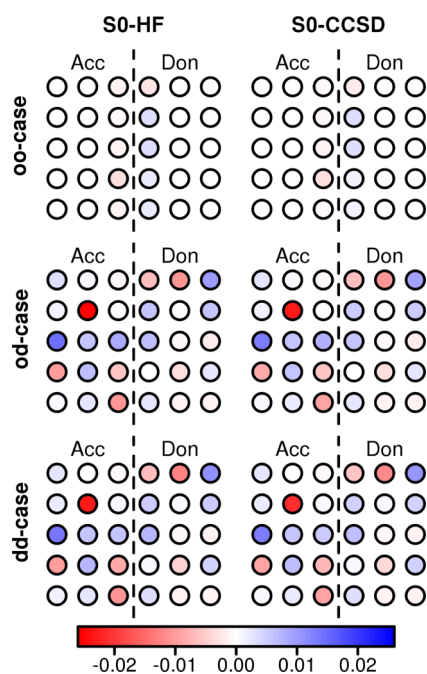


**Figure 4.** Ground-state HF (left) and CCSD (right) charges in the model two-dimensional heterojunctions.

letter indicates diagonal order, the second one off-diagonal order), phases with diagonal order and off-diagonal disorder (od-case), and phases with both diagonal and off-diagonal disorder (dd-case).<sup>33</sup> We have assumed that the D–A orbital couplings are disordered even when the individual phases are ordered because epitaxial matching between two crystalline phases is the exception rather than the rule. Table III, together with Table II for the on-site part of the Hamiltonian, summarizes the input parameters of these calculations. Again, these are to some extent arbitrary, but they are quite reasonable for typical materials. A more systematic exploration of different parameter combinations would be necessary and interesting, but this is a long task that we leave for the future.

Figure 4 illustrates the charges on the sites of the model heterojunctions calculated from the HF and CCSD ground-state wave functions. A few points are worth noting. The first one is the almost perfect agreement between the HF and CCSD charges. This confirms that the HF method already provides a very good description of the ground state in both ordered and disordered situations. At the interface between two ordered phases (oo-case), we observe the formation of a very weak interfacial dipole. The overall charge on either side of the interface is only  $\pm 0.008$  electrons. This weak dipole is in apparent contradiction with recent work of Linares et al.<sup>34</sup> on the pentacene–C<sub>60</sub> interface. In that work, however, it was demonstrated that the calculated interfacial dipole does not originate from a partial charge transfer from the donor to the

acceptor but rather from polarization effects that are not included in our model. After the introduction of the off-diagonal disorder (od-case), we observe a certain tendency to charge localization in some energetically favorable sites. There is of course a large body of literature on disordered systems, random matrices, and the Anderson localization that is relevant in this context.<sup>35</sup> The sites where charge concentrates are not necessarily those next to the interface, and indeed there are also some small positive charges within the A phase and some negative ones in the D phase. However, the overall charge within the D and A phases is almost unchanged ( $\pm 0.008$  electrons). The further introduction of on-diagonal disorder (dd-case with  $\sigma_w = \sigma_b$ , Table III) apparently has little effect on the charge distribution. The overall charge on the two sides of the interface is now  $\pm 0.010$ . We point out that all these calculations have been purposely carried out with the same random number seed in order to compare systems with identical portions of the one-electron Hamiltonian. These calculations would have to be repeated several times with different seeds in order to accumulate some statistics on different realizations of the disorder.

Table IV collects the electron correlation energies extracted from the CCSD calculations. The correlation energies for a

**Table IV.** Electron Correlation Energies from CCSD Calculations on Two-Dimensional Systems (absolute values, in eV)

	oo-case	od-case	dd-case
A–D heteroj.	0.965	0.947	0.951
All-A	1.431	1.400	1.418
All-D	0.499	0.496	0.502

given system (all-A, all-D, or heterojunction) are almost independent of disorder, as this represents a relatively weak perturbation. There are, however, important differences between the two phases. We see that electron correlation is much more important in the acceptor than in the donor. The D–A heterojunction has an intermediate behavior, probably due to a simple averaging effect. All this demonstrates that even though correlation effects appeared to be negligible on the basis of the ground-state charges (Figure 4), this might not be completely true in general. We plan to return to this question and address it more thoroughly in the future.

The promotion of one electron from the 30 occupied to the 30 unoccupied HF orbitals within the two-dimensional arrays leads to exactly 900 singlet and 900 triplet excited states. All these can be readily obtained by a CIS calculation, and Figure 5 presents the resulting DOSs. Both single-phase systems have an almost Gaussian DOS, respectively, centered around 2.5 eV (A) and 3.0 eV (D). The width of these DOSs increases appreciably upon introduction of off-diagonal disorder. By comparison, on-diagonal disorder produces only an additional minor

**Table III.** Parameters ( in eV) for the One-Electron Hamiltonian in Two-Dimensional Systems<sup>a</sup>

	all calculations			oo-case		od-case		dd-case	
	$t_{HH}^0$	$t_{HL}^0$	$t_{LL}^0$	$\sigma_w$	$\sigma_t$	$\sigma_w$	$\sigma_t$	$\sigma_w$	$\sigma_t$
A phase	0.08	0.04	−0.08	0.00	0.00	0.00	0.08	0.08	0.08
D phase	0.08	−0.04	−0.08	0.00	0.00	0.00	0.08	0.08	0.08
A–D interface	0.00	0.00	0.00	–	0.08	–	0.08	–	0.08

<sup>a</sup>In all calculations,  $\epsilon_r = 3.5$ ,  $D = 3.5$  Å, and  $R_0 = 10$  Å (eq 24).

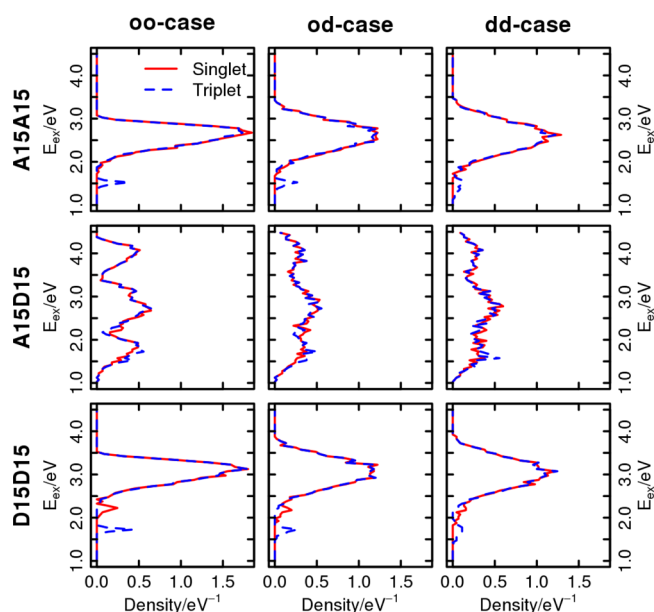


**Figure 5.** Density-of-states from CIS calculations on all-A (top), A–D (middle), and all-D (bottom) two-dimensional systems of 30 sites.

perturbation, in agreement with our previous discussion of the ground-state charge distributions. The predominance of the off-diagonal disorder is at first surprising, but it might be quite simply related to the greater number of off-diagonal elements in a large matrix (their number scales as  $\sim N^2$  instead of  $N$ ). This was observed also in a recent study of the one-electron levels in model paracrystalline materials.<sup>36</sup> The distributions of singlet and triplet excitation are rather similar, except for the presence of a triplet peak at low energies (1.5–2.0 eV).

The D–A heterojunctions have a radically different DOS. In the ordered system (oo-case), this can be described as the superposition of three or perhaps four Gaussians. The lower energy one (1.0–2.0 eV) corresponds to electron transfer excitations from D to A (Figure 6), the middle one (2.0–3.5 eV) to excitations within the single phases, and the higher energy one (3.5–4.5 eV) to electron transfer from A to D. The introduction of disorder broadens and merges these peaks within the DOS. Again, the off-diagonal disorder appears to be more significant than the diagonal one. The distributions of singlet and triplet excited states appear to be almost superposable in these heterojunctions.

Finally, Figure 6 illustrates the charge distributions within the first excited singlet and triplet states of the heterojunctions. In all the studied systems, these occur at about 1.1 eV. They all involve the transfer of almost exactly one electron from the donor to the acceptor phase. The singlet and triplet charge distributions are almost identical. This is understandable because we have two essentially unpaired electrons within distinct phases. We observe charge delocalization in the oo-case and localization in the od-case and dd-case. It is surprising that in these two cases there is virtually no charge within the two layers of A and D sites forming the interface. Thus, the lowest energy excitations in these disordered systems already produce a very loosely bound electron–hole pair. In other words, we seem to have found a striking example of long-range electron transfer, similar to that recently discussed by Troisi.<sup>12</sup>

Further calculations on larger systems are currently being performed in order to exclude finite-size effects and accumulate statistically significant data on the latter point. Figure 7 presents

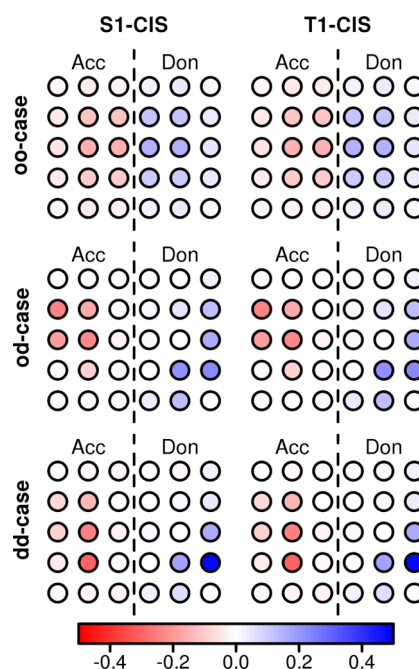


**Figure 6.** Charges in the first excited singlet (left) and triplet (right) states from the CIS calculations on the two-dimensional heterojunctions. Note the change in the color scale with respect to Figure 4.

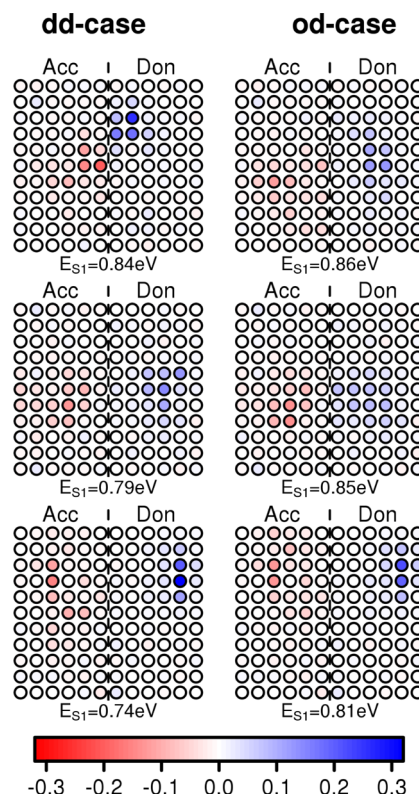


**Figure 7.** Charges in the first excited singlet states from CIS calculations on two-dimensional heterojunctions consisting of 66 D and 66 A sites. The corresponding excitation energies are also indicated.

some preliminary results on a few two-dimensional heterojunctions containing 132 sites. These have been generated with different random number seeds for the one-electron Hamiltonian, all other parameters being equal to those used for the



smaller arrays (Table III). In fact, they have been selected by us in order to highlight the possibility of different scenarios. We see that depending on the specific realization of the disorder the charges extracted from the first singlet excited state may be more or less delocalized, as well as more or less “bound” to each other at the donor–acceptor interface. Notice also that there is a certain spread in the calculated excitation energies. Thus, these calculations confirm the possibility of long-range electron transfer, but highlight also the need of a more systematic study. This should include also other low-energy excited states, in addition to the first one.

## VI. SUMMARY AND CONCLUSIONS

We have developed and implemented a coarse-grained quantum chemical model of organic semiconducting materials, which is based on an effective Hamiltonian with just two electrons and two orbitals per molecule/site. The model can be parametrized for specific systems, and it provides a consistent semiquantitative treatment of their ground, ionized, and excited states. It covers an interesting middle ground between all-atom quantum chemical models, which at the moment can only be used on “small” systems of  $\approx 10^2$  atoms, and models such as kinetic Monte Carlo or microelectrostatics that are essentially based on localized “classical” descriptions of the charges/excitons and their interactions. The model does not assume localization or delocalization of the electronic wave functions; hence, it is equally applicable to both ordered and disordered systems. Although it has been developed with photovoltaic applications in mind, it is sufficiently general to be useful also for other organic electronics materials and applications.

The simplicity of the model allows very fast calculations and greatly facilitates the interpretation of the results. All the calculations presented here were carried out on a laptop computer, and we may thus expect to study much larger ones by moving to parallel supercomputers. The calculations have already provided evidence for the possibility of low-energy, long-range, electron transfer in donor–acceptor heterojunctions characterized by a moderate degree of disorder. More systematic calculations are now being performed in order to assess the role of different variables in a statistically meaningful way. For the sake of simplicity, positional disorder of the sites has been neglected in the present calculations. It could have been included within the present model in a straightforward way, but we avoided it in order to keep the number of model parameters to a minimum and, similarly, for the possibility of a composition and/or disorder gradient in the direction orthogonal to the interface.

Our approach could certainly benefit from further validation studies and methodological extensions. For example, it would be interesting to know whether it can be meaningfully applied to realistic configurations of conjugated molecules extracted from atomistic or coarse-grained simulations. At the very least, this would require the use of one-electron Hamiltonian parameters from density functional, *ab initio*, or semiempirical quantum chemical calculations.<sup>24,25</sup> The assumption of roughly spherical sites might have to be lifted in order to deal with systems characterized by strong global or local anisotropy, such as liquid crystals or long conjugated polymer segments. Polarization effects resulting from molecular dipoles (and higher electrostatic moments) have been neglected here, even though other studies have shown that they can be significant under certain circumstances.<sup>34,37</sup> It would be interesting to include them, but this has to be done carefully in order to retain

consistency with the continuum electrostatic description adopted here.

## AUTHOR INFORMATION

### Corresponding Author

\*E-mail: guido.raos@polimi.it.

### Notes

The authors declare no competing financial interest.

## ACKNOWLEDGMENTS

G.R. thanks Mario Raimondi for introducing him to quantum chemistry several years ago. This work was supported by the Fondazione Cariplo through Grant 2011-0349 (PLENOS project).

## REFERENCES

- (1) (a) Nelson, J. *Mater. Today* **2011**, *14*, 462–470. (b) Li, G.; Zhu, R.; Yang, Y. *Nature Photon* **2012**, *6*, 153–161.
- (2) (a) Brédas, J.-L.; Norton, J. E.; Cornil, J.; Coropceanu, V. *Acc. Chem. Res.* **2009**, *42*, 1691–1699. (b) Zhu, X.-Y.; Yang, Q.; Muntwiler, M. *Acc. Chem. Res.* **2009**, *42*, 1779–1187. (c) Clarke, T. M.; Durrant, J. R. *Chem. Rev.* **2010**, *110*, 6736–6767. (d) Nayak, P. K.; Narasimhan, K. L.; Cahen, D. *J. Phys. Chem. Lett.* **2013**, *4*, 1707–1717.
- (3) (a) Nelson, J.; Kwiatkowski, J. J.; Kirkpatrick, J.; Frost, J. M. *Acc. Chem. Res.* **2009**, *42*, 1768–78. (b) Difley, S.; Wang, L.-P.; Yeganeh, S.; Yost, S. R.; Van Voorhis, T. *Acc. Chem. Res.* **2010**, *43*, 995–1004. (c) Beljonne, D.; Cornil, J.; Muccioli, L.; Zannoni, C.; Brédas, J.-L.; Castet, F. *Chem. Mater.* **2011**, *23*, 591–609.
- (4) (a) Kanai, Y.; Grossman, J. C. *Nano Lett.* **2007**, *7*, 1967–1972. (b) Yi, Y.; Coropceanu, V.; Brédas, J.-L. *J. Am. Chem. Soc.* **2009**, *131*, 15777–15783. (c) Liu, T.; Troisi, A. *J. Phys. Chem. C* **2011**, *115*, 2406–2415. (d) McMahon, D. P.; Cheung, D. L.; Troisi, A. *J. Phys. Chem. Lett.* **2011**, *2*, 2737–2741. (e) Yost, S. R.; Van Voorhis, T. *J. Phys. Chem. C* **2013**, *117*, 5617–5625. (f) D’Avino, G.; Mothy, S.; Muccioli, L.; Zannoni, C.; Wang, L.; Cornil, J.; Beljonne, D.; Castet, F. *J. Phys. Chem. C* **2013**, *117*, 12981–12990.
- (5) (a) Huang, D. M.; Moule, A. J.; Faller, R. *Fluid Phase Equilib.* **2011**, *302*, 21–25. (b) Lee, C.-K.; Pao, C.-W.; Chu, C.-W. *Energy Env. Sci.* **2011**, *4*, 4124–4132.
- (6) (a) Rivnay, J.; Mannsfeld, S. C. B.; Miller, C. E.; Salleo, A.; Toney, M. F. *Chem. Rev.* **2012**, *112*, 5488–5519. (b) Liu, F.; Gu, Y.; Jung, J. W.; Jo, W. H.; Russell, T. P. *J. Polym. Sci. B: Polym. Phys.* **2012**, *50*, 1018–1044.
- (7) (a) Anta, J. A. *Energy Env. Sci.* **2009**, *2*, 387–392. (b) Meng, L.; Shang, Y.; Li, Q.; Li, Y.; Zhan, X.; Shuai, Z.; Kimber, R. G. E.; Walker, A. B. *J. Phys. Chem. B* **2010**, *114*, 36–41. (c) Groves, C.; Kimber, R. G. E.; Walker, A. B. *J. Chem. Phys.* **2010**, *133*, 144110–1/7. (d) Casalegno, M.; Raos, G.; Po, R. *J. Chem. Phys.* **2010**, *132*, 094705–1/14.
- (8) (a) Houili, H.; Tutiš, E.; Batistiš, I.; Zuppiroli, L. *J. Appl. Phys.* **2006**, *100*, 033702–1/12. (b) Einax, M.; Dierl, M.; Nitzan, A. *J. Phys. Chem. C* **2011**, *115*, 21396–21401. (c) Xu, F.; Yan, D. *Appl. Phys. Lett.* **2011**, *99*, 113303–1/3. (d) Casalegno, M.; Bernardi, A.; Raos, G. *J. Chem. Phys.* **2013**, *139*, 024706–1/13.
- (9) (a) Barker, J. A.; Ramsdale, C. M.; Greenham, N. C. *Phys. Rev. B* **2003**, *67*, 075205. (b) Koster, L. J. A.; Mihailetschi, V. D.; Ramaker, R.; Blom, P. W. M. *Appl. Phys. Lett.* **2005**, *86*, 123509. (c) Koster, L. J. A.; Smits, E. C. P.; Mihailetschi, V. D.; Blom, P. W. M. *Phys. Rev. B* **2005**, *72*, 085205. (d) De Falco, C.; Porro, M.; Sacco, R.; Verri, M. *Comput. Methods Appl. Math.* **2012**, *102*, 245–246.
- (10) (a) Lyons, B. P.; Clarke, N.; Groves, C. *Energy Env. Sci.* **2012**, *5*, 7657. (b) Donets, S.; Pershin, A.; Christlmaier, M. J.; Baeurle, S. A. *J. Chem. Phys.* **2013**, *138*, 094901.
- (11) Smith, M. B.; Michl, J. *Chem. Rev.* **2010**, *110*, 6891–6936.
- (12) (a) Caruso, D.; Troisi, A. *Proc. Natl. Acad. Sci. U.S.A.* **2012**, *109*, 13498–13502. (b) Troisi, A. *Faraday Discuss.* **2013**, *163*, 377–392.
- (13) Savoie, B. M.; Jackson, N. E.; Marks, T. J.; Ratner, M. A. *Phys. Chem. Chem. Phys.* **2013**, *15*, 4538–4547.



- (14) McWeeny, R. *Methods of Molecular Quantum Mechanics*, 2nd ed.; Academic Press: London, 1989; Chapter 3.
- (15) Pople, J. A.; Beveridge, D. L. *Approximate Molecular Orbital Theory*; McGraw-Hill: New York, 1970; Chapter 2.
- (16) Schatz, G. C.; Ratner, M. *Quantum Mechanics in Chemistry*; Dover Publications: New York, 2002; Chapter 6.
- (17) Note that  $h_{12}^0$  must be zero, for otherwise, the singly excited configuration would mix with the ground-state wave function.
- (18) For simplicity, in eq 3, we have written the electron–core interactions as if the latter consisted of a single point charge. In reality, the contribution to the one-electron Hamiltonian by a molecule at  $\mathbf{R}_k$  should involve both an electrostatic interaction with several nuclei and a Coulomb-plus-exchange interaction with a core electron density  $\rho_k^c(\mathbf{r})$ . This is implicitly taken care of by our parametrization scheme.
- (19) The theory can be developed also without this approximation, but it requires as input further experimental data, such as the excitation energies of the cation and anion. This extension will be given a future publication.
- (20) (a) Sassara, A.; Zerza, G.; Chergui, M. *J. Phys. Chem. A* **1998**, *102*, 3072–3077. (b) Boltalina, O.; Ioffe, I.; Sidorov, L. N.; Seifert, G.; Vietze, K. *J. Am. Chem. Soc.* **2000**, *122*, 9745–9749. (c) Orlandi, G.; Negri, F. *Photochem. Photobiol. Sci.* **2002**, *1*, 289–308.
- (21) We use  $C_{70}$  instead of  $C_{60}$  as a prototypical A-type material because the very high symmetry of the latter implies a high degree of orbital degeneracy. This would complicate the application of our model. For the same reason,  $C_{70}$  can be considered more representative of other lower-symmetry materials (see ref 20c).
- (22) (a) Schmidt, W. *J. Chem. Phys.* **1977**, *66*, 828–845. (b) Crocker, L.; Wang, T.; Kebabian, P. *J. Am. Chem. Soc.* **1993**, *115*, 7818–7822. (c) Halasinski, T.; Hudgins, D.; Salama, F.; Allamandola, L. J.; Bally, T. *J. Phys. Chem. A* **2000**, *104*, 7484–7491. (d) Hajgató, B.; Szieberth, D.; Geerlings, P.; De Proft, F.; Deleuze, M. *S. J. Chem. Phys.* **2009**, *131*, 224321.
- (23) Bässler, H. *Phys. Status Solidi B* **1993**, *175*, 15–56.
- (24) (a) Newton, M. D. *Chem. Rev.* **1991**, *91*, 767–792. (b) Brédas, J.-L.; Beljonne, D.; Coropceanu, V.; Cornil, J. *Chem. Rev.* **2004**, *104*, 4971–5004. (c) Hsu, C. *Acc. Chem. Res.* **2009**, *42*, 509–518.
- (25) (a) Troisi, A. *Adv. Mater.* **2007**, *19*, 2000–2004. (b) Fratini, S.; Ciuchi, S. *Phys. Rev. Lett.* **2009**, *103*, 266601. (c) Rühle, V.; Lukyanov, A.; May, F.; Schrader, M.; Vehoff, T.; Kirkpatrick, J.; Baumeier, B.; Andrienko, D. *J. Chem. Theory Comput.* **2011**, *7*, 3335–3345. (d) Oberhofer, H.; Blumberger, J. *Phys. Chem. Chem. Phys.* **2012**, *14*, 13846–13852.
- (26) Tomasi, J.; Mennucci, B.; Cammi, R. *Chem. Rev.* **2005**, *105*, 2999–3093.
- (27) In principle, also the excited states of the neutral molecule could be affected by the surrounding dielectric. However, the effect would be certainly weaker, and it would depend on the ground- and excited-state dipole moments. Because dipole moments are not an ingredient of our model, it seems both reasonable and theoretically consistent to neglect this effect, at least for the moment.
- (28) (a) Born, M. *Z. Phys.* **1920**, *1*, 45. (b) Israelachvili, J. *Intermolecular and Surface Forces*, 3rd ed.; Academic Press: San Diego, 2010.
- (29) (a) Schmidt, M. W.; Baldridge, K. A.; Boatz, J. A.; Elbert, S. T.; Gordon, M. S.; Jensen, J. H.; Koseki, S.; Matsunaga, N.; Nguyen, K. A.; Su, S. J.; Windus, T. L.; Dupuis, M.; Montgomery, J. A. *J. Comput. Chem.* **1993**, *14*, 1347–1363. (b) Gordon, M. S.; Schmidt, M. W. *Advances in Electronic Structure Theory: GAMESS a Decade Later. In Theory and Applications of Computational Chemistry, the First 40 years; Dykstra, C. E., Frenking, G., Lim, K. S., Scuseria, G. E., Eds.; Elsevier: Amsterdam, 2005.*
- (30) Dreuw, A.; Head-Gordon, M. *Chem. Rev.* **2005**, *105*, 4009–4037.
- (31) Ivanic, J.; Ruedenberg, K. *J. Chem. Phys.* **2003**, *119*, 9364–9376.
- (32) (a) Bartlett, R.; Musial, M. *Rev. Mod. Phys.* **2007**, *79*, 291–352. (b) Piecuch, P.; Kucharski, S. A.; Kowalski, K.; Musial, M. *Comput. Phys. Commun.* **2002**, *149*, 71–96.
- (33) We do not present calculations on a hypothetical “do-case” because it is difficult to conceive a practical situation with diagonal disorder and off-diagonal order.
- (34) Linares, M.; Beljonne, D.; Cornil, J.; Lancaster, K.; Brédas, J.-L.; Fuchs, A.; Lennartz, C.; Idé, J.; Méreau, R.; Aurel, P.; Ducasse, L.; Castet, F. *J. Phys. Chem. C* **2010**, *114*, 3215–3224.
- (35) (a) Lee, P. A.; Ramakrishnan, T. V. *Rev. Mod. Phys.* **1985**, *57*, 287–337. (b) Skinner, J. L. *J. Phys. Chem.* **1994**, *98*, 2503–2507. (c) Papenbrock, T.; Weidenmüller, H. *A. Rev. Mod. Phys.* **2007**, *79*, 997–1013.
- (36) Noriega, R.; Rivnay, J.; Vandewal, K.; Koch, F. P. V.; Stingelin, N.; Smith, P.; Toney, M. F.; Salleo, A. *Nat. Mater.* **2013**, *12*, 1038–1044.
- (37) May, F.; Baumeier, B.; Lennartz, C.; Andrienko, D. *Phys. Rev. Lett.* **2012**, *109*, 136401–1/5.